ELSEVIER

Contents lists available at ScienceDirect

# Matrix Biology

journal homepage: www.elsevier.com/locate/matbio





# Transglutaminase-mediated stiffening of the glomerular basement membrane mitigates pressure-induced reductions in molecular sieving coefficient by reducing compression

Dan Wang, Nicholas Ferrell

Department of Internal Medicine, Division of Nephrology, The Ohio State University Wexner Medical Center, 1664 Neil Ave. 4th Floor, Suite 4100, Columbus, OH 43201, United States

#### ARTICLE INFO

Keywords:
Glomerular basement membrane
Molecular permeability
Sieving coefficient
Stiffness
Elastic modulus
Crosslinking

#### ABSTRACT

Proteinuria, the presence of high molecular weight proteins in the urine, is a primary indicator of chronic kidney disease. Proteinuria results from increased molecular permeability of the glomerular filtration barrier combined with saturation or defects in tubular protein reabsorption. Any solute that passes into the glomerular filtrate traverses the glomerular endothelium, the glomerular basement membrane, and the podocyte slit diaphragm. Damage to any layer of the filter has reciprocal effects on other layers to increase glomerular permeability. The GBM is thought to act as a compressible ultrafilter that has increased molecular selectivity with increased pressure due to compression that reduced the porosity of the GBM with increased pressure. In multiple forms of chronic kidney disease, crosslinking enzymes are upregulated and may act to increase GBM stiffness. Here we show that enzymatically crosslinking porcine GBM with transglutaminase increases the stiffness of the GBM and mitigates pressure-dependent reductions in molecular sieving coefficient. This was modeled mathematically using a modified membrane transport model accounting for GBM compression. Changes in the mechanical properties of the GBM may contribute to proteinuria through pressure-dependent effects on GBM porosity.

#### Introduction

The kidney glomerulus has the ability to efficiently filter the blood and allow high permeability of water and low molecular weight solutes while retaining large molecular weight proteins such as albumin in the circulation. Under normal physiological conditions, little protein crosses the capillary wall, and the small amount that does is captured and processed by the proximal tubule epithelium [1]. In the setting of kidney disease, loss of glomerular size selectivity and/or saturation or defects in proximal tubular reabsorption leads to proteinuria and passage of large molecular weight proteins in the urine [2]. Proteinuria is a primary indicator of progressive renal damage and is associated with a high risk of adverse events including end stage kidney disease, cardiovascular disease, and death [3,4]. Despite the importance of glomerular function to maintaining homeostasis, the precise mechanisms that regulate glomerular permeability in health and the factors that contribute to proteinuria in disease are not fully understood.

The glomerular capillary wall consists of the glomerular endothelium, the glomerular basement membrane (GBM), and the podocytes.

The degree to which each layer of the glomerular filtration barrier contributes to overall molecular permeability and how the overall structure works in concert to restrict protein transport remains an active area of investigation [5–9]. Damage to any component of the filter can lead to loss of selectivity, and damage to one structure can affect the function of adjacent layers [10–13]. This suggests that each component of the filtration barrier is important for overall function and crosstalk between different layers is important for maintaining proper function.

The GBM serves as a physical barrier to passage of protein across the kidney filtration barrier [14–17]. Studies of macromolecular transport in isolated basement membranes, including the GBM, show that they act as gel-like compressible filters with more stringent size selectivity and reduced hydraulic permeability at higher transmembrane pressures [15, 18–20]. This is illustrated schematically in Fig. 1. Recently, the gel compression model of glomerular filtration has been revisited to encompass the role of podocytes in providing a buttressing force against filtration pressure. Studies by Butt et al. observed that in podocin mutant mice, reductions in glomerular filtration rate were less than what would be expected based on the reduction in filtration area in the setting of

E-mail address: ferrell.61@osu.edu (N. Ferrell).

<sup>\*</sup> Corresponding author.

podocyte effacement [21,22]. Based on mathematical modeling, they showed that an increase in hydraulic permeability due to loss of podocyte forces and reduced GBM compression could account for this effect. Under this paradigm, healthy podocytes act as a buttress against the pressure drop across the glomerular capillary wall and allow the GBM to compress against the podocytes. In disease, podocyte architecture and cytoskeletal structure are compromised and do not provide a sufficient buttressing force effectively increasing the hydraulic and molecular permeability of the filtration barrier. Under this model, the mechanical properties of the GBM are inherently important as stiffness defines the degree of compressibility of the basement membrane under applied pressure.

Chronic kidney disease (CKD) is characterized by increased extracellular matrix (ECM) crosslinking through both enzymatic and nonenzymatic mechanisms. Crosslinking enzymes including tissue transglutaminase (TGM2) and lysyl oxidases (LOX) play a role in multiple chronic kidney diseases. TGM2 expression and activity are increased in CKD, and genetic knockout or pharmacological inhibitors of TGM2 protect against kidney fibrosis in CKD and diabetic kidney disease [23-27]. LOX like 2 (LOXL2) is an important GBM crosslinking enzyme [28] and inhibition of LOXL2 protects against multiple forms of CKD [29,30]. Diabetic kidney disease is characterized by increased non-enzymatic crosslinking through formation of advanced glycation end-products (AGEs) [31,32]. We previously showed that glycation of the glomerular ECM ex vivo increases the stiffness of the ECM [33,34]. In the setting of increased crosslinking, stiffening of the GBM would be expected to reduce compressibility and could result in increased permeability at a given pressure. Additionally, crosslink inhibitors could potentially preserve the compressibility of the native GBM to mitigate proteinuria in the setting of chronic disease. Experimentally, effects of biochemical modifications of the GBM through chemical crosslinking or sugar modification have been mixed. Chemically induced crosslinking increased GBM permeability ex vivo [18]. Daniels and Hauser showed that sugar modification of albumin increased its permeability, but direct sugar modification of the GBM did not affect permeability [35]. Here we aimed to determine how biochemical modification of the GBM with an enzymatic crosslinker affects mechanical properties of the GBM and how this would alter its pressure-dependent permeability. We hypothesized that the degree of molecular crosslinking of the basement membranes is an important determinant of pressure-dependent permeability through changes in the biomechanical properties of the basement membrane that reduce membrane compression. To test this hypothesis, we used microbial transglutaminase (mTG) to crosslink the GBM, and diffusive and

convective molecular transport properties of the GBM were measured *ex vivo*. A mathematical model based on modified membrane transport theory to account for compression effects was used to evaluate GBM sieving coefficient in native and enzymatically crosslinked GBM. This analysis confirmed that native GBM exhibits increased molecular selectivity with applied pressure, and this effect is mitigated in transglutaminase crosslinked GBM.

#### Results

Glomerular isolation and characterization

Isolated glomeruli were characterized by visual inspection during the isolation and decellularization procedure. Glomeruli were enriched during the isolation procedure. Decellularized glomeruli were intact and retained their structure following decellularization (Fig. 2A). Decellularized glomeruli and GBM membranes were further characterized by SEM (Fig. 2B and 2C). Isolated and decellularized GBM were free of any obvious cell debris and GBM from individual glomerular capillaries are visible in the electron micrographs.

## mTG treatment increases GBM stiffness

To determine the effects of mTG mediated crosslinking on GBM stiffness, decellularized glomeruli were subjected to compressive loading using a custom compression system as described previously [33, 34] following mTG treatment. The mechanism of mTG mediated crosslinking and characterization of purified mTG are shown in Supplementary Fig. S1. The purified mTG was evaluated using Coomassie Blue staining. The results showed a single band with an expected molecular weight of ~38 kDa. Decellularized glomeruli were held in place with microcapillary tubing attached to a syringe to apply a vacuum (Fig. 3A). Glomeruli were compressed against a calibrated microcantilever to measure the force versus displacement ( $\delta/R$ ), where  $\delta$  is the change in radius and R is the original radius. mTG treatment resulted in a dose dependent upward shift in the force versus displacement ( $\delta/R$ ) response (Fig. 3B). GBM treated with collagenase (1 mg/mL) showed the opposite trend with a time dependent decrease in GBM stiffness with increasing duration of collagenase treatment (Supplementary Fig. S2). Force displacement response was curve fit to a Tatara model for compression of a sphere and elastic modulus (E) was calculated as a model fit parameter. This analysis showed a dose-dependent increase in elastic modulus with increasing mTG concentration (Fig. 3C). Untreated

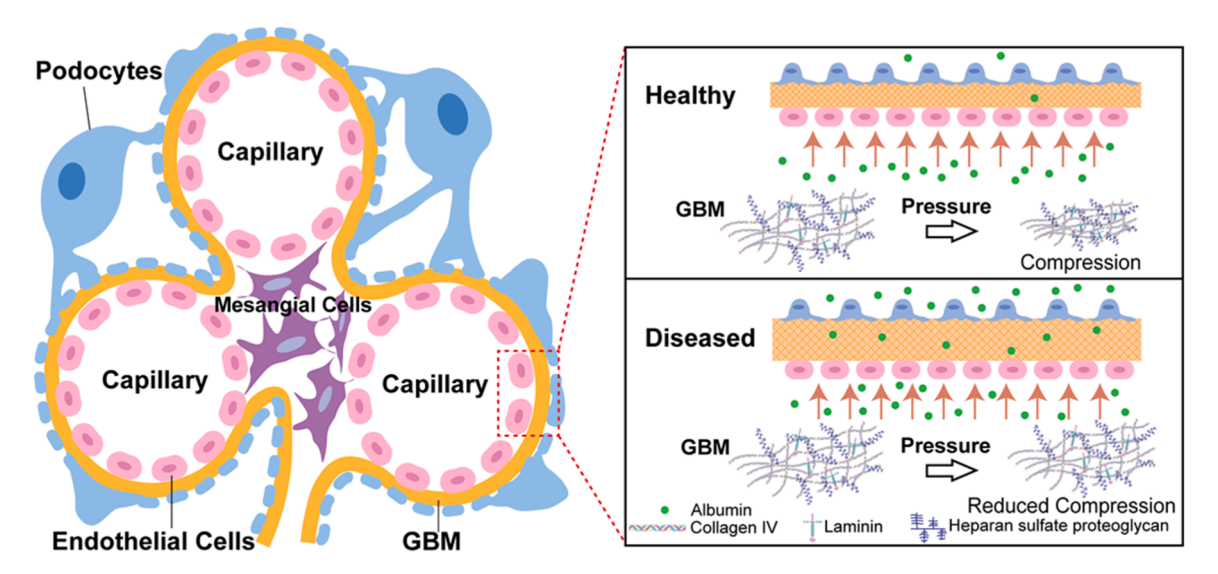
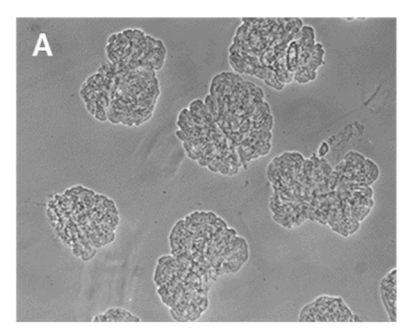
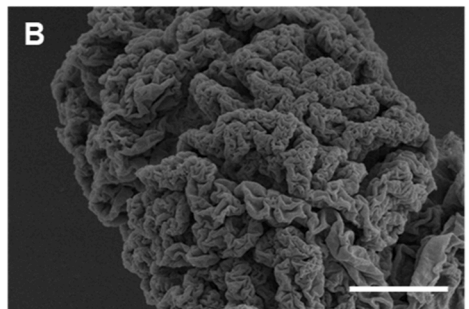


Fig. 1. Schematic of pressure-dependent compression of the GBM in health and disease. Under healthy conditions, the GBM compresses under pressure to restrict protein transport. In disease, the GBM is crosslinked and stiffened to reduce pressure induced compression and increase molecular permeability.





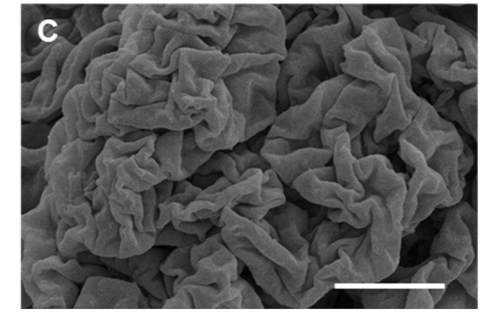


Fig. 2. Characterization of isolated decellularized glomeruli. (A) Decellularized glomeruli were imaged under a Widefield microscope. (B,C) Scanning electron micrographs of decellularized glomerular basement membrane (scale bars are  $15 \mu m$  and  $5 \mu m$ , respectively).

glomeruli had a modulus of approximately 50 Pa and stiffness increased by approximately 4-fold in glomeruli treated with 100  $\mu$ g/mL mTG. There was a statistically significant increase in stiffness for all of the mTG concentrations (5, 25, 50, and 100  $\mu$ g/mL) as compared to the untreated control.

## mTG effects on diffusional permeability

To evaluate the effects of crosslinking on diffusive permeability, FITC-Ficoll (1 mg/mL) was added to the apical side of the GBM, and time-dependent change in Ficoll concentration was measured on the basal side of the membrane. The diffusive permeability decreased as a function of increasing molecular radius, indicative of restricted diffusion with increased molecular size (Fig. 4A). mTG treatment (100 µg/mL) resulted in a small reduction in diffusive permeability. This suggests that mTG crosslinking slightly reduced the pore size of the GBM. The diffusive hindrance factor, ( $\Phi$ Kd)0, of native and mTG crosslinked GBM were calculated according to Eq. (7). The experimental data and model curve fits at  $r_s$ =3–7 nm are shown in Fig. 4B. The results show that the model fits were in good agreement with the experimental data.

# GBM stiffening mitigates pressure-dependent compression effects on molecular permeability

Sieving coefficients of native and mTG-treated (100 µg/mL) GBM were evaluated under 0.5, 1.5, and 2.5 psi pressure. The results showed that the native GBM exhibited pressure-dependent characteristics with a reduction in sieving coefficient with increasing pressure. This effect was significantly reduced in crosslinked GBM, resulting in higher molecular sieving coefficients in mTG treated GBM at higher pressure relative to native GBM (Fig. 5). As the pressure increased from 0.5 to 2.5 psi, the molecular cutoff ( $\Theta$ <0.1) of native GBM decreased from 6.54±0.16 nm to 4.96±0.16 nm in native GBM. In contrast, the mTG-treated GBM showed only a slight decrease in molecular cutoff with a mean of 7.05  $\pm 0.29$  nm at 0.5 psi and  $6.57\pm 0.38$  nm at 2.5 psi. There was no significant difference in molecular cutoff between native and mTG-treated GBM at low pressure (0.5 psi), but a significant difference arises at 1.5 and 2.5 psi (Fig. 5B and 5C). This indicates that native GBM demonstrates pressure-dependent reductions in molecular transport at higherpressure conditions, whereas such behavior is not observed in stiffened GBM.

To further evaluate the pressure-dependent effect on native and mTG-treated GBM, the sieving coefficients of native and mTG-treated GBM at 0.5, 1.5, and 2.5 psi pressure were compared at  $r_s = 2$  nm, 4 nm, and 6 nm, respectively (Fig. 6). At  $r_s = 2$  nm (Fig. 6A), the sieving coefficient of native GBM significantly decreased from  $0.80\pm0.02$  at 0.5 psi to  $0.67\pm0.03$  at 2.5 psi, while the mTG-treated GBM slightly reduced from  $0.83\pm0.02$  to  $0.71\pm0.05$ . Similarly, the sieving coefficient of native GBM decreased significantly from  $0.51\pm0.03$  to  $0.23\pm0.02$  at  $r_s = 4$  nm (Fig. 6B), while it dropped from  $0.15\pm0.02$  to  $0.04\pm0.01$  at  $r_s = 6$  nm (Fig. 6C). However, the sieving coefficient of mTG-treated GBM

were  $0.52\pm0.03$  at 0.5 psi and  $0.41\pm0.06$  at 2.5 psi at  $r_s$ =4 nm, and  $0.19\pm0.02$  to  $0.17\pm0.04$  at  $r_s$ =6 nm, with none of the differences reaching statistical significance. This indicates that the native GBM exhibits a pressure-induced reduction in molecular sieving coefficient due to membrane compression while this effect is mitigated in mTG crosslinked GBM

#### Mathematical modeling of sieving coefficients

To further evaluate pressure-dependent effects of native and mTGtreated GBM, we employed a mathematical model of the molecular sieving coefficient (Eqs. (3)-(6)). The modeled diffusive hindrance factor for native GBM was  $(\Phi K_d)_0 = 0.072 \cdot \exp(-0.64 \cdot r_s)$ , which is comparable to the results  $(\Phi K_d)_0 = 0.11 \cdot \exp(-0.73 \cdot r_s)$  measured previously by Edwards et al. as well as our previous results evaluating diffusive permeability of isolated GBM [15]. The modeled diffusive hindrance factor for mTG treated GBM is  $(\Phi K_d)_0 = 0.048 \cdot \exp(-0.59 \cdot r_s)$ , which is similar to the hindrance factor of native GBM. The pressure-dependent fit parameter in native GBM was  $\beta$ =0.001 indicating that the sieving coefficient is dependent on applied pressure in native GBM (Fig. 7A). The sieving coefficient modeled on mTG-treated GBM did not show a pressure-dependent effect, where  $\beta$ =1  $\times$  10<sup>-5</sup> (Fig. 7B). The estimated convective hindrance factor of native and mTG treated GBM are  $(\Phi K_c)_0 = 1.086 \cdot \exp(-0.41 \cdot r_s)$  and  $(\Phi K_c)_0 = 1.199 \cdot \exp(-0.29 \cdot r_s)$ , respectively.

#### Discussion

Multiple biological hydrogels and basement membranes, including the GBM, act as compressible membranes with more stringent molecular selectivity with increasing pressure [15,18-20]. As transmembrane pressure increases, membrane compression reduces the effective porosity and limits molecular transport. This effect in the glomerular capillary wall is illustrated schematically in Fig. 1 where native GBM is able to compress against podocytes under normal filtration pressure to reduce the effective pore size to enhance molecular selectivity. In the setting of disease-mediated excessive crosslinking, the GBM is unable to compress under filtration pressure to increase the sieving coefficient under applied pressure. We tested this hypothesis in isolated porcine GBM crosslinked with mTG. We assume based on the high degree of size selectivity, that the transport properties of the decellularized glomeruli are dominated by the GBM, but the mesangial matrix is present and may contribute to the overall molecular permeability. Pig kidneys were chosen because glomeruli could be isolated in large numbers using a simple size-based technique. Multiple ECM crosslinking enzymes including transglutaminase and lysyl oxidases have been shown to be upregulated in different forms of chronic kidney disease such as diabetic nephropathy and in the setting of kidney fibrosis. We chose microbial transglutaminase as a crosslinking agent because it acts via a similar crosslinking mechanism to tissue transglutaminase but can be isolated in

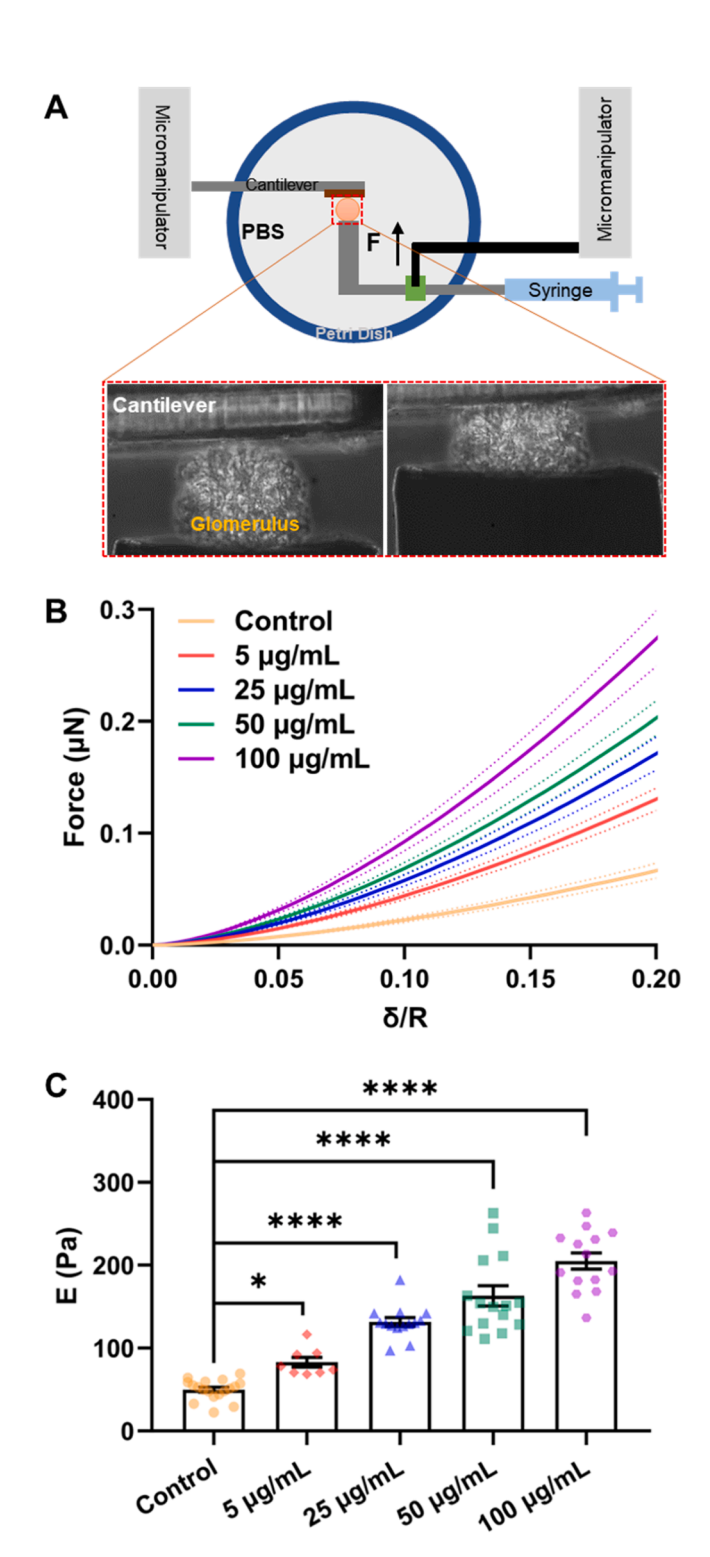
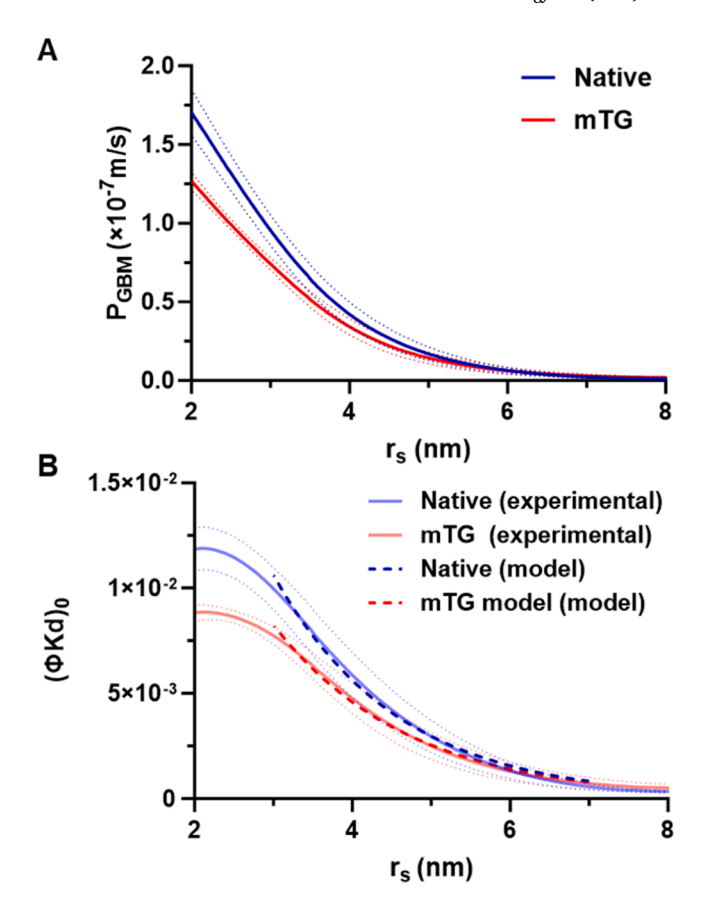


Fig. 3. mTG treatment increases the stiffness of decellularized glomeruli. (A) Schematic drawing of the experimental setup. (B) Experimental data fit to Hertz-Tatara model after glomeruli incubated in mTG for 24 h. (C) Stiffness of native and mTG crosslinked glomeruli at a concentration of 0, 5, 25, 50, and 100  $\mu g/mL$  after 24 h incubation. Data are shown at the mean±SEM. Statistical significance was determined by one-way ANOVA with Dunnett's post-hoc testing for comparison of mTG treatment versus control. \* $p<0.05,\ ****p<0.0001,\ n=18,\ 8,\ 14,\ 15,\ and\ 14$  for 0, 5, 25, 50, and 100  $\mu g/mL$  mTG, respectively.



**Fig. 4.** Diffusive Ficoll transport properties of native and mTG treated (100  $\mu$ g/mL) GBM (A) Ficoll permeability (P<sub>GBM</sub>) of GBM (n=7). (B) Diffusive hindrance factors for native the mTG modified GBM with exponential fit to experimental data for  $r_s$  from 3 to 7 nm.

large quantities from a commercial source at low cost [36]. Microbial transglutaminase has been widely used as a crosslinking agent for modifying biomaterial properties for tissue engineering and drug delivery applications [37–40].

Multiple decellularization strategies have been explored for organ and tissue decellularization. These include sodium dodecyl sulfate (SDS), Triton-X 100, and sodium deoxycholate (SDC) [41]. We chose SDC because it effectively removed cellular components from glomeruli while preserving the overall ultrastructure of the GBM as shown in the SEM images (Fig. 2). We cannot rule out that the decellularization protocol removes molecular components of the GBM that may be relevant to molecular transport properties. The GBM is known to be compositionally complex and consists of many structural, signaling, and ECM associated molecular components that may alter the structure and/or charge of the GBM [42]. We have shown previously that SDS based decellularization of GBM and tubular basement membrane does remove some laminin, but significant amounts of collagen IV and laminin are retained in the decellularized ECM [17,34,43]. Any decellularization strategy is likely to remove some molecular constituents of the GBM, and a balance of effective removal of cellular protein with retention of GBM components is needed. Based on the preserved molecular selectivity following decellularization, it appears that many of the structural components that impart the GBM with its molecular selectivity are retained following SDC-based decellularization.

We developed a cantilever-based compression assay for evaluating the compressive stiffness of glomeruli. Using this technique, we showed that sugar-meditated glycation and crosslinking increases glomerular ECM stiffness *ex vivo* [33]. While physiologically relevant, this reaction is relatively slow requiring weeks to months to crosslink the ECM with

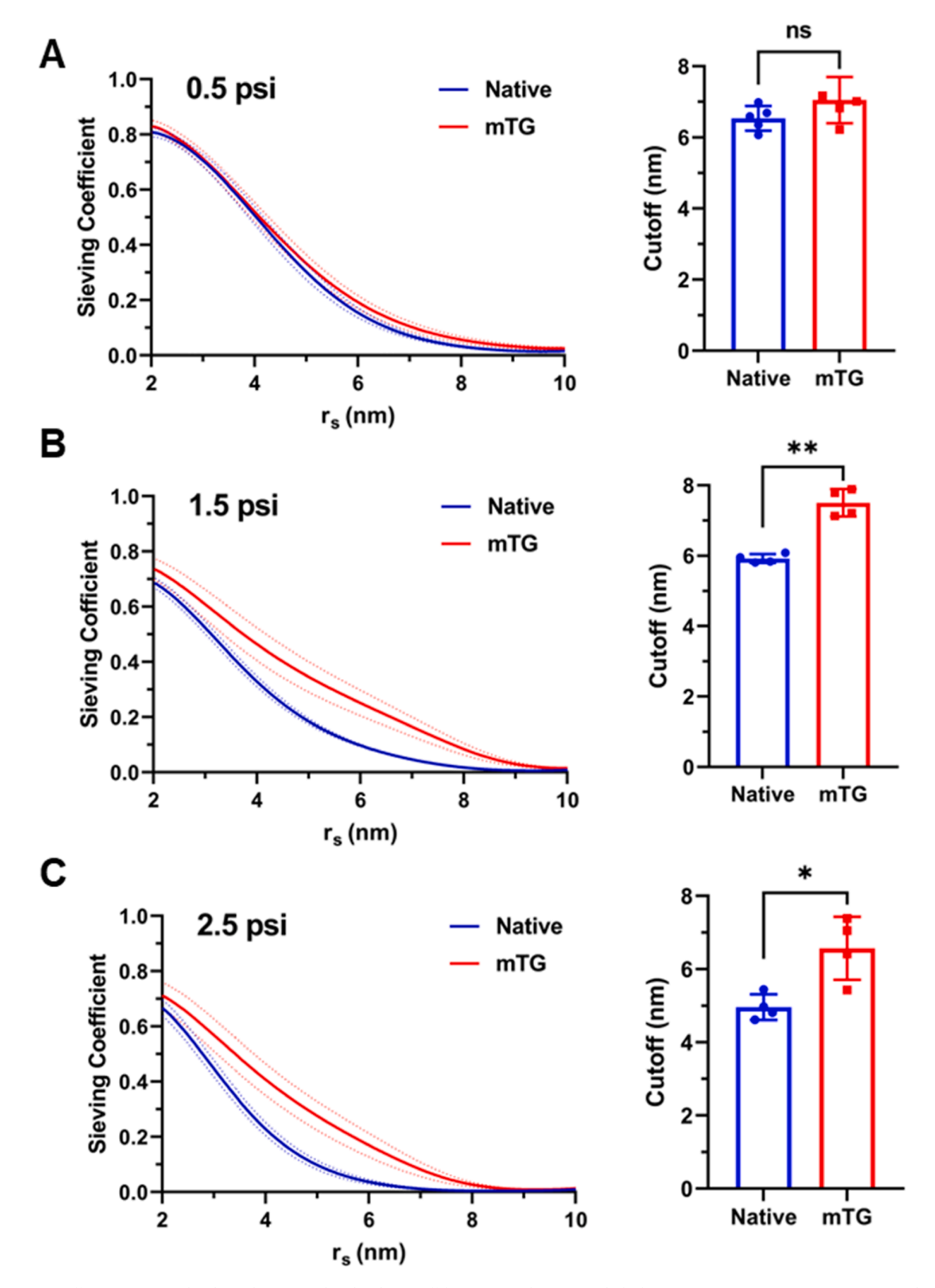
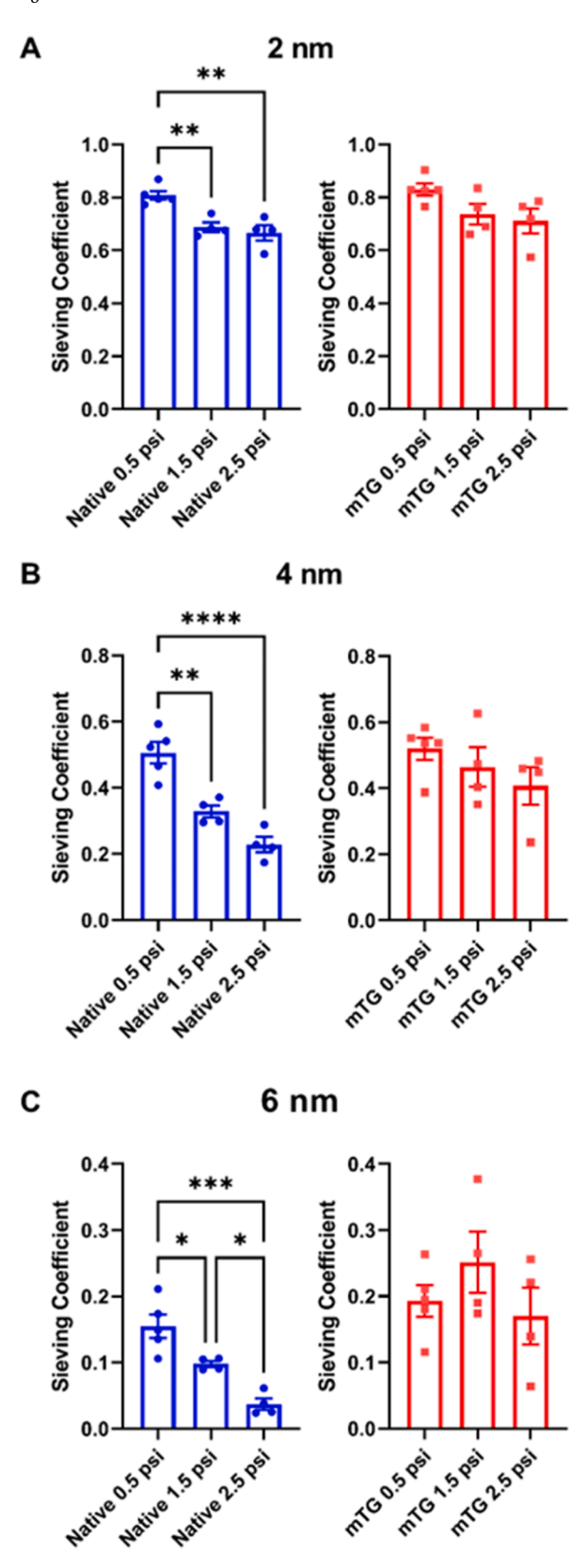
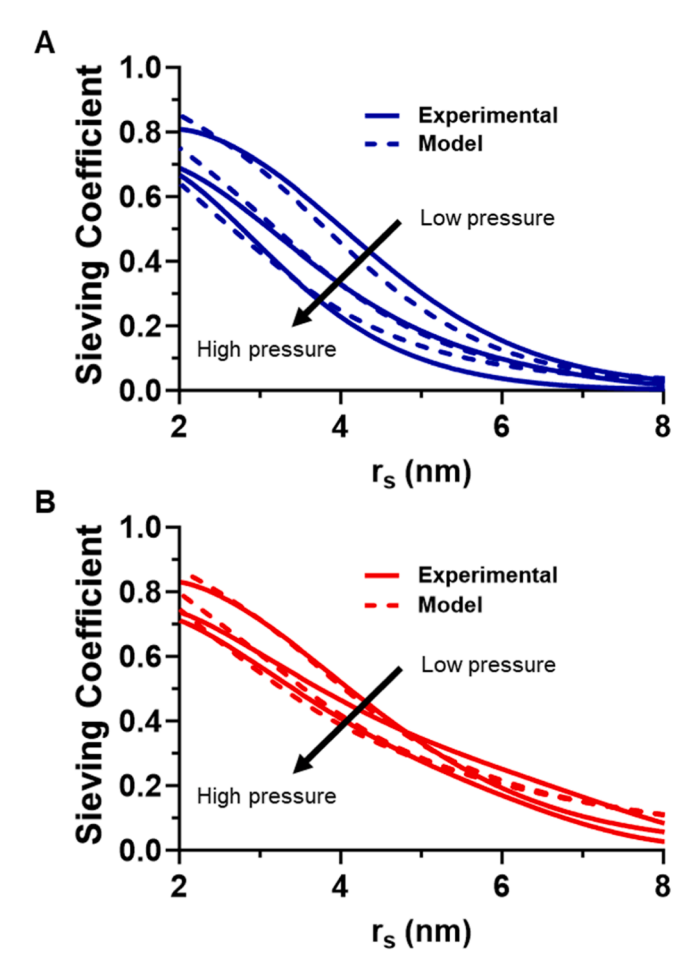


Fig. 5. Sieving coefficient versus molecular radius ( $r_s$ ) and molecular cutoff for native and mTG crosslinked (100  $\mu$ g/mL) GBM at (A) 0.5, (B) 1.5, and (C) 2.5 psi. Differences in molecular cutoff of native and crosslinked GBM were analyzed by paired *t*-test, \*p < 0.5, \*\*p < 0.01, ns=nonsignificant, n = 4-5 replicates per condition.



**Fig. 6.** Comparison of sieving coefficient measured on (A) native and (B) mTG treated GBM at 0.5, 1.5, and 2.5 psi with  $r_s$ =2 nm, 4 nm, and 6 nm. Statistical analyses are determined by one-way ANOVA with Tukey post-hoc test. \*p < 0.05, \*\*p < 0.01, \*\*\*p < 0.001, \*\*\*p < 0.0001, p = 4–5 replicates per condition.



**Fig. 7.** Mathematical modeling of Ficoll sieving coefficient across the GBM at 0.5, 1.5, and 2.5 psi. (A) Model fit was in excellent agreement with experimental data in native GBM and compression effects were needed to optimize the model fit. (B) Compression effects were lost in mTG modified GBM and pressure effects did not significantly improve the fit for crosslinked GBM.

reducing sugars. Enzymatic crosslinking is also relevant to several pathophysiological settings, but the reaction is rapid. Here we show that mTG crosslinking increases GBM stiffness after 24 h in a dose dependent manner (Fig. 3). Crosslinking of GBM with the same mTG concentration for 4 days resulted in a similar increase in GBM stiffness but plateaued at  $25 \, \mu g/mL \, mTG$  (Supplementary Fig. S3).

Intuitively, one could consider that crosslinking of basement membrane would render them more selective by reducing the porosity through formation of intermolecular crosslinks. In fact, this does occur to a small degree with regard to diffusive transport in response to mTG crosslinking (Fig. 4) as well as chemical crosslinking of other basement membrane systems [43]. However, this effect was minimal and was observed only for small molecular weight solutes.

More pronounced effects of crosslinking on molecular transport are observed in the setting of applied pressures that span the physiological to pathophysiological range. At low pressure, the sieving coefficient of native and mTG treated GBM was relatively similar. In both cases, the GBM provides a stringent barrier to Ficoll transport with a steady reduction in sieving coefficient with increasing molecular radius and a molecular cutoff ( $\Theta$ <0.1) of approximately 6–7 nm and a slight but not statistically significant (p=0.13) increase in molecular cutoff in the mTG treated GBM (Fig. 5). Similar to trends seen in previous studies of GBM and other basement membrane systems [15,19,20], increased pressure resulted in improved molecular selectivity in native GBM with reduction in molecular sieving coefficient in native GBM at multiple molecular radii (Fig. 6). This effect was mitigated in mTG crosslinked

GBM. There were trends toward reduced sieving coefficient in mTG treated GBM at 2 and 4 nm (Fig. 6A and 6B), but did not reach statistical significance suggesting that crosslinked GBM is not completely incompressible but is significantly less as compared to native GBM. Differences in sieving coefficient at 1.5 and 2.5 psi were also blunted in native GBM and only reached statistical significance for 6 nm radius Ficoll (Fig. 6C). This further substantiated the non-linear relationship between applied pressure and compression indicative of strain stiffening.

While the GBM provides a stringent barrier to passage of Ficoll at size ranges relevant to glomerular filtration, the molecular sieving coefficient is larger than the in vivo glomerular sieving coefficient. This is not unexpected given the importance of podocytes in regulating glomerular filtration and the likely reciprocal relationship between podocytes and the GBM in determining glomerular permeability. Additionally, the sieving coefficient of Ficoll is larger than the sieving coefficient of globular proteins such as albumin of an equivalent hydrodynamic radius [44,45]. This has been attributed to differences in size, shape, flexibility and charge of Ficoll relative to globular proteins. Negatively charged Ficoll exhibits a lower sieving coefficient both in vivo and with various in vitro basement membrane systems [46,47]. Ficoll also exhibits a higher than expected sieving coefficient in monodisperse nanoporous membranes suggesting that it does not behave as a rigid spherical molecule [48]. These studies establish that Ficoll acts as a broad molecular weight tracer with a molecular size that is relevant to glomerular permeability, but the absolute sieving coefficient should be taken in the context of Ficoll's hyperpermeability relative to globular proteins such as albumin of an equivalent molecular radius.

Established membrane transport theory was in excellent agreement with experimental data for native basement membranes (Fig. 7) with pressure induced reductions in GBM sieving coefficient being accounted for by both an increase in Peclet number at increased solvent flux and pressure-dependent compression that alters diffusive and convective hindrance factors with increased transmembrane pressure. This effect was significantly mitigated in stiff, crosslinked GBM and compression effects had minimal effect on the model fit to the experimental data. These data confirm previous studies showing that GBM acts as a compressible filter with increased selectivity with increased pressure. We established a direct relationship between GBM stiffness and loss of compression effects using a physiologically relevant enzymatic crosslinking mechanism.

#### Conclusion

We hypothesized that crosslinking of GBM using mTG would increase the elastic modulus and reduce compression effects on Ficoll sieving coefficient. To test this hypothesis, we measured the stiffness of isolated GBM following treatment with mTG. This analysis confirmed that enzymatic crosslinking significantly increased GBM stiffness in a dose dependent manner. This biochemical modification has only a marginal effect on passive diffusion of Ficoll across the GBM but has a significant effect in the presence of applied pressure. Under pressure, Ficoll sieving coefficient decreased as a function of increased pressure as expected for a compressible ultrafilter. This effect was lost in mTG treated GBM. These data point to potential effects of disease mediated stiffening of the GBM as a molecular mechanism contributing to loss of glomerular size selectivity in the setting of chronic kidney disease.

#### Materials and methods

## Microbial transglutaminase purification

Native GBM was crosslinked with mTG (ACTIVA TI; Ajinomoto) derived from  $Streptomyces\ mobaraensis$ . The mTG was purified by cation exchange chromatography using an SP Sepharose column (HiTrap, 5 mL). The column was pre-equilibrated with 50 mL buffer A (20 mM sodium phosphate, 2 mM ethylenediaminetetraacetic acid disodium salt

dihydrate, pH 6.0) at a flow rate of 2 mL/min. To purify mTG, 10 g ACTIVA TI was dissolved in 100 mL buffer A followed by centrifugation at 5000 rpm for 5 min. The supernatant was loaded onto the column at the same flow rate. After washing the column with 50 mL of buffer A, mTG was eluted with buffer B (buffer A with 800 mM NaCl, pH 6.0). Approximately 5 mL purified mTG was collected after discarding the first 4 mL of flow through. The mTG was desalted using a PD-10 column (17085101, GE Healthcare). The PD-10 column was pre-equilibrated with 0.22  $\mu$ m filtered phosphate buffer (50 mM phosphate, 150 mM NaCl, pH 7.0). After adding mTG to the column, the purified and desalted mTG was eluted. The mTG concentration was determined by a BCA protein assay kit (Pierce). The enzyme was aliquoted and stored at  $-20~^{\circ}$ C.

# GBM preparation

Pig kidneys were obtained from Lampire Biological Laboratories or a local slaughterhouse. Glomeruli were isolated on ice. After slicing the tissue with an electric food slicer, kidney cortex was minced using razor blades. The tissue was then passed through a 250 µm sieve using a 60 mL syringe plunger. Ice-cold PBS was frequently added to the tissue to assist in passing through the sieves. Glomeruli were then passed through a 150  $\mu m$  sieve and collected on a 32  $\mu m$  sieve. Glomeruli were decellularized with 1 % SDC in deionized water (dH<sub>2</sub>O) with daily changes until no residual protein was observed (5-7 days). Following decellularization, the glomeruli were pelleted by centrifugation and washed with dH2O water for two days (5 times per day) without disturbing the pellet. The decellularized glomeruli were used for stiffness measurements or lyophilized for long-term storage at -80 °C. For diffusional permeability assays, lyophilized glomeruli were sonicated in PBS (250 µL, 10 mg/mL) and consolidated on a Transwell insert (0.4 µm, 12-well plate, Corning) in a 3 mL stirred cell for 30 min at 259 mmHg (5 psi) air pressure as described previously [17]. A nylon mesh and an O-ring were attached to the back side of the Transwell filter to prevent membrane damage. Transwell inserts with GBM were sterilized with 0.18 % peracetic acid (PAA) and 4.8 % ethanol in dH<sub>2</sub>O for 30 min. The GBM was washed with sterile PBS five times per day for 2 days. For the pressure-dependent compression assays, filter paper (GB003, Whatman GE Healthcare) and a supporting membrane (PBVK02510, EMD Millipore) were layered and assembled at the base of the stirred cell as described previously [49]. The supporting membrane had a nominal molecular weight limit (NMWL) of 500 kDa. GBM solution, 300 µL, was added to the stirred cell and consolidated under 259 mmHg pressure for 3 h.

# Scanning electron microscopy (SEM) sample preparation

Decellularized glomeruli were washed with  $dH_2O$  five times, followed by fixation with 4 % paraformaldehyde. The glomeruli were washed with  $dH_2O$  and then sequentially incubated with 50 %, 70 %, 90 %, and 100 % ethanol for 10 min each. Coverslips (12 mm, round) were coated with 2 % gelatin (G7041, Sigma-Aldrich) in  $dH_2O$  at 37 °C for 30 min. Approximately 50  $\mu L$  of the solution containing glomeruli was added to each coverslip. The coverslips were left undisturbed for a few minutes until the glomeruli were firmly attached to the surface. The samples were dried using a Pelco critical point drier before gold sputtering coating. Images were taken by SEM (Thermo Scientific Apreo).

#### Stiffness measurements on decellularized glomeruli

The stiffness of native and mTG-crosslinked glomeruli was characterized using a cantilever-based compression system as described previously [33]. Decellularized glomeruli were washed with dH<sub>2</sub>O and incubated with 0–100  $\mu$ g/mL mTG in PBS for 24 h. As a negative control, a set of glomeruli were treated with 1 mg/mL collagenase type 4 (LS004188, Worthington Biochemical) in Hank's Balanced Salt Solution with calcium and magnesium (14025076, Gibco) for 5, 15, and 30 min

at 37 °C. Glomeruli were vacuum fixed to chromatography tubing (25  $\mu m$  inner diameter) using a 10 mL syringe. A customized cantilever with a spring constant of 10 nN/ $\mu m$  was fabricated from a glass capillary tube by a pipette puller. The cantilever displacement was controlled by a micromanipulator at a speed of 5  $\mu m/sec$ . Displacement of the cantilever and deformation of the glomerulus were analyzed using WINanalyze software. The measured force-displacement responses were fit to a modified Tatara model to calculate elastic modulus as described previously [33].

## FITC-Ficoll preparation and characterization

FITC-Ficoll labeling and characterization were performed as described previously [47,50,51], and a detailed preparation and analysis protocol can be found in Wang et al. [49]. Briefly, 100 mg Ficoll PM 70 (F2878, Sigma Aldrich) was dissolved in 1.9 mL dimethyl sulfoxide (DMSO) at 37 °C in a water bath for 20 min to facilitate dissolution. FITC (46424, Thermo Fisher) was dissolved at 100 mg/mL in DMSO with 20 mg/mL sodium bicarbonate. 100  $\mu$ L of FITC-sodium bicarbonate was added to Ficoll solution to bring the total volume to 2 mL and was boiled in water for 15 min. The FITC-Ficoll was precipitated by adding 20 mL absolute ethanol overnight protected from light. Then FITC-Ficoll was pelleted and resuspended in 2 mL dH<sub>2</sub>O and placed in a water bath for 20 min for dissolution. A PD-10 column (17085101, GE Healthcare) was used to remove unbound FITC after column equilibration according to the manufacturer's instructions.

FITC-Ficoll concentration was determined by size exclusion chromatography in an Agilent 1260 Infinity II HPLC system using an Ultrahydrogel 500 column (PSS831913, Waters). The flow rate of 0.22  $\mu m$  filtered mobile phase (50 mM phosphate, 150 mM NaCl, 0.01% w/v sodium azide in dH<sub>2</sub>O, pH 7.0) was 0.5 mL/min. FITC-Ficoll (10  $\mu L$ ) was injected and analyzed by a fluorescence detector (G7121A, Agilent) at excitation/emission 495/520. Ficoll concentration versus molecular radius was analyzed in MATLAB.

#### Diffusional permeability assays

To evaluate the effects of crosslinking on diffusive molecular transport, native GBM was crosslinked with 100  $\mu$ g/mL sterile mTG in sterile PBS for 24 h in a 37 °C incubator. Crosslinked GBM was washed with sterile PBS five times to remove residual enzyme. To perform diffusional permeability assays, the apical compartment of the GBM was filled with 0.5 mL of 1 mg/mL FITC-Ficoll. The basolateral compartment was filled with 1.5 mL PBS only. A 100  $\mu$ L sample was collected from the basolateral side at 30 and 60 min. To measure the diffusive permeability of Transwell filter only ( $P_{TM}$ ) the sample was collected at 5 and 15 min after diffusion. The concentration of the apical solution did not change significantly during the course of the experiment (Supplementary Fig. S4). Diffusional permeability was determined by Eq. (1) as described previously [47].

$$P_{GBM+TM} = -\ln \left[ \frac{C_B(t) - C_A}{C_B(0) - C_A} \right] \cdot \frac{V}{At}$$
 (1)

where  $C_B(t)$  and  $C_B(0)$  are the concentrations in the basolateral compartment at two time points after diffusion, respectively;  $C_A$  is the concentration of the apical compartment;  $P_{GBM+TM}$  is the diffusive permeability of the GBM and the Transwell support; A is the area of the membrane; and V is the volume of the basal compartment.

The diffusional permeability of the GBM ( $P_{GBM}$ ) was calculated using Eq. (2) to take into account the contribution of the Transwell membrane diffusive permeability ( $P_{TM}$ )

$$\frac{1}{P_{GBM+TM}} = \frac{1}{P_{GBM}} + \frac{1}{P_{TM}}$$
 (2)

Pressure-dependent molecular sieving

To determine the effects of crosslinking and stiffening of GBM on pressure-dependent molecular sieving, FITC-Ficoll in PBS (3 mL, 0.1 mg/mL) was injected into the stirred cell. Air pressure at 26, 78, and 129 mmHg (0.5, 1.5 and 2.5 psi) was applied to the GBM to drive fluid and molecular flux across the membrane. After obtaining the first 200 µL of filtrate, 500 µL of fresh FITC-Ficoll solution was injected into the stirred cell. After mixing, 300 µL of Ficoll solution was removed from the stirred cell and was used as the feed solution. The process was repeated until three filtrate and feed samples were obtained. After measuring the sieving coefficient, the native GBM was incubated with 2 mL 100 µg/mL mTG in PBS at 40 °C on a hotplate. The assays were conducted on the same GBM substrate before and after crosslinking. The FITC-Ficoll feed and filtrate samples were analyzed by size exclusion chromatography as described above. The sieving coefficient ( $\theta$ ) was calculated as the ratio of the filtrate concentration (C<sub>Filtrate</sub>) over the feed concentration (C<sub>Feed</sub>) by  $\theta = C_{Filtrate}/C_{Feed}$ .

#### Mathematical model of compression dependent molecular sieving

To model the pressure-dependent effects of FITC-Ficoll sieving coefficient we used a similar approach to that described by Edwards et al. [15] with a modified term to describe membrane compression effects. The molecular sieving coefficient is described by Eqs. (3)–(5))

$$\theta = \frac{\Phi K_c}{1 - (1 - \Phi K_c) \exp(-Pe)} \tag{3}$$

$$Pe = \frac{(\Phi K_c)\nu\delta}{\Phi K_d D_m} \tag{4}$$

$$D_{\infty} = \frac{\kappa T}{6\pi \eta r_{\rm s}} \tag{5}$$

where  $\Phi K_c$  and  $\Phi K_d$  are the convective and diffusive hindrance factors, respectively, Pe is the Peclet number,  $\nu$  is the fluid viscosity,  $\delta$  is the thickness,  $D_\infty$  is the free diffusivity,  $\kappa$  is Boltzmann's constant, T is absolute temperature, and  $\eta$  is solvent viscosity. To account for membrane compressibility, Edward et al. assumed a linear reduction in  $\Phi K_c$  and  $\Phi K_d$  with increasing pressure [15]. We have observed non-linear dependence between applied force and GBM displacement indicative of strain stiffening or increased stiffness at increase applied stress [33, 34]. As such, we reasoned that the dependence of the hindrance factors would be more pronounced at lower pressures and reduced as pressure increases due to strain stiffening. Therefore, we defined the dependence of  $\Phi K_c$  and  $\Phi K_d$  on pressure as

$$\frac{\Phi K_d}{(\Phi K_d)_0} = 1 - e^{-\beta \Delta P} = \frac{\Phi K_c}{(\Phi K_c)_0} \tag{6}$$

$$P_{GBM} = \frac{\Phi K_d D_{\infty}}{\delta} \tag{7}$$

where  $(\Phi K_d)_0$  and  $(\Phi K_c)_0$  are the diffusive and convective hindrance factors at zero pressure.  $(\Phi K_d)_0$  was determined experimentally from the measured diffusive permeability  $(P_{GBM})$  at molecular radii from 3 to 7 nm according to Eq. (7) where  $\delta$  is the membrane thickness. The pressure dependence parameter  $\beta$  and  $(\Phi K_c)_0$  were fit to the experimental sieving coefficient data by least square error analysis in Matlab.  $(\Phi K_d)_0$  was modeled as  $(\Phi K_d)_0 = a \cdot \exp(-b \cdot r_s)$ , and  $(\Phi K_c)_0$  was modeled as  $(\Phi K_c)_0 = d \cdot \exp(-e \cdot r_s)$  [17].

## Statistical analysis

The results are presented as the mean  $\pm$  standard error of the mean (SEM). Statistical comparisons were made using paired *t*-test, unpaired *t*-

test, or one-way ANOVA with Dunnett's or Tukey post-hoc test. Statistical tests were performed with GraphPad Prism. A p value <0.05 was considered statistically significance.

## Declaration of competing interest

The authors declare no conflicts of interest.

#### Data availability

Data will be made available on request.

#### Acknowledgments

This research was funded by a CAREER Award (2216394) from National Science Foundation (to N.F.) and a Ben J. Lipps Research Fellowship Award from American Society of Nephrology (to D.W.). Imaging support was provided by the OSU Center for Electron Microscopy. We acknowledge resources from the Campus Microscopy and Imaging Facility (CMIF) and the OSU Comprehensive Cancer Center (OSUCCC) Microscopy Shared Resource (MSR), The Ohio State University. This facility is supported in part by grant P30 CA016058, National Cancer Institute, Bethesda, MD.

## Supplementary materials

Supplementary material associated with this article can be found, in the online version, at doi:10.1016/j.matbio.2024.05.002.

#### References

- [1] M. Gekle, Renal tubule albumin transport, Annu. Rev. Physiol. 67 (2005) 573-594.
- [2] G. D'amico, C. Bazzi, Pathophysiology of proteinuria, Kidney Int. 63 (3) (2003) 809–825.
- [3] B.R. Hemmelgarn, et al., Relation between kidney function, proteinuria, and adverse outcomes, JAMA 303 (5) (2010) 423–429.
- [4] K. Zandi-Nejad, A.A. Eddy, R.J. Glassock, B.M. Brenner, Why is proteinuria an ominous biomarker of progressive kidney disease? Kidney Int. 66 (2004) S76–S89.
- [5] W.H. Fissell, J.H. Miner, What is the glomerular ultrafiltration barrier? J. Am. Soc. Nephrol. 29 (9) (2018) 2262–2264.
- [6] M.C. Menon, P.Y. Chuang, C.J. He, The glomerular filtration barrier: components and crosstalk, Int. J. Nephrol. 2012 (2012) 749010.
- [7] G. Jarad, J.H. Miner, Update on the glomerular filtration barrier, Curr. Opin. Nephrol. Hypertens. 18 (3) (2009) 226–232.
- [8] I.S. Daehn, J.S. Duffield, The glomerular filtration barrier: a structural target for novel kidney therapies, Nat. Rev. Drug Discov. 20 (10) (2021) 770–788.
- [9] M.G. Farquhar, The primary glomerular filtration barrier-basement membrane or epithelial slits? Kidney Int. 8 (4) (1975) 197–211.
- [10] A. Singh, et al., Glomerular endothelial glycocalyx constitutes a barrier to protein permeability, J. Am. Soc. Nephrol. 18 (11) (2007) 2885–2893.
- [11] S.D. Funk, M.H. Lin, J.H. Miner, Alport syndrome and Pierson syndrome: diseases of the glomerular basement membrane, Matrix Biol. 71-72 (2018) 250–261.
- [12] G. Jarad, J. Cunningham, A.S. Shaw, J.H. Miner, Proteinuria precedes podocyte abnormalities inLamb2-/-mice, implicating the glomerular basement membrane as an albumin barrier, J. Clin. Investig. 116 (8) (2006) 2272–2279.
- [13] J. Patrakka, K. Tryggvason, New insights into the role of podocytes in proteinuria, Nat. Rev. Nephrol. 5 (8) (2009) 463–468.
- [14] J.H. Suh, J.H. Miner, The glomerular basement membrane as a barrier to albumin, Nat. Rev. Nephrol. 9 (8) (2013) 470–477.
- [15] A. Edwards, B.S. Daniels, W.M. Deen, Hindered transport of macromolecules in isolated glomeruli. II. Convection and pressure effects in basement membrane, Biophys. J. 72 (1) (1997) 214–222.
- [16] A. Edwards, W.M. Deen, B.S. Daniels, Hindered transport of macromolecules in isolated glomeruli. I. Diffusion across intact and cell-free capillaries, Biophys. J. 72 (1) (1997) 204–213.
- [17] D. Wang, S. Sant, N. Ferrell, A biomimetic in vitro model of the kidney filtration barrier using tissue-derived glomerular basement membrane, Adv. Healthc. Mater. 10 (16) (2021) 2002275.
- [18] H.A. Walton, J. Byrne, G.B. Robinson, Studies of the permeation properties of glomerular basement membrane: cross-linking renders glomerular basement membrane permeable to protein, Biochim. Biophys. Acta 1138 (3) (1992) 173–183.
- [19] W.H. Fissell, et al., Solute partitioning and filtration by extracellular matrices, Am. J. Physiol. Ren. Physiol. 297 (4) (2009) F1092–F1100.

[20] B.S. Daniels, E.B. Hauser, W.M. Deen, T. Hostetter, Glomerular basement membrane: in vitro studies of water and protein permeability, Am. J. Physiol. Ren. Physiol. 262 (6) (1992) F919–F926.

- [21] L. Butt, et al., A molecular mechanism explaining albuminuria in kidney disease, Nat. Metab. 2 (5) (2020) 461–474.
- [22] T. Benzing, D. Salant, Insights into glomerular filtration and albuminuria, N. Engl. J. Med. 384 (15) (2021) 1437–1446.
- [23] T.S. Johnson, et al., Tissue transglutaminase and the progression of human renal scarring, J. Am. Soc. Nephrol. 14 (8) (2003) 2052–2062.
- [24] T.S. Johnson, et al., Transglutaminase inhibition reduces fibrosis and preserves function in experimental chronic kidney disease, J. Am. Soc. Nephrol. 18 (12) (2007) 3078–3088.
- [25] L. Huang, et al., Transglutaminase inhibition ameliorates experimental diabetic nephropathy, Kidney Int. 76 (4) (2009) 383–394.
- [26] N. Shweke, et al., Tissue transglutaminase contributes to interstitial renal fibrosis by favoring accumulation of fibrillar collagen through TGF-β activation and cell infiltration, Am. J. Pathol. 173 (3) (2008) 631–642.
- [27] A.A. Satoskar, et al., Differentiating Staphylococcus infection-associated glomerulonephritis and primary IgA nephropathy: a mass spectrometry-based exploratory study, Sci. Rep. 10 (1) (2020) 17179.
- [28] C. Añazco, et al., Lysyl oxidase-like-2 cross-links collagen IV of glomerular basement membrane, J. Biol. Chem. 291 (50) (2016) 25999–26012.
- [29] D. Cosgrove, et al., Lysyl oxidase like-2 contributes to renal fibrosis in Col4α3/ Alport mice, Kidney Int. 94 (2) (2018) 303–314.
- [30] S. Stangenberg, et al., Lysyl oxidase-like 2 inhibition ameliorates glomerulosclerosis and albuminuria in diabetic nephropathy, Sci. Rep. 8 (1) (2018) 9423
- [31] D.R. Sell, et al., Glucosepane is a major protein cross-link of the senescent human extracellular matrix: relationship with diabetes, J. Biol. Chem. 280 (13) (2005) 12310–12315.
- [32] J.M. Bohlender, S. Franke, G. Stein, G. Wolf, Advanced glycation end products and the kidney, Am. J. Physiol. Ren. Physiol. 289 (4) (2005) F645–F659.
- [33] S. Sant, D. Wang, R. Agarwal, S. Dillender, N. Ferrell, Glycation alters the mechanical behavior of kidney extracellular matrix, Matrix Biol. Plus 8 (2020) 100035.
- [34] S. Sant, D. Wang, M. Abidi, G. Walker, N. Ferrell, Mechanical characterization of native and sugar-modified decellularized kidneys, J. Mech. Behav. Biomed. Mater. 114 (2021) 104220.
- [35] B.S. Daniels, E.B. Hauser, Glycation of albumin, not glomerular basement membrane, alters permeability in an in vitro model, Diabetes 41 (11) (1992) 1415–1421.
- [36] Y. Zhu, J. Tramper, Novel applications for microbial transglutaminase beyond food processing, Trends Biotechnol. 26 (10) (2008) 559–565.
- [37] S.K. Chan, T.S. Lim, Bioengineering of microbial transglutaminase for biomedical applications, Appl. Microbiol. Biotechnol. 103 (7) (2019) 2973–2984.
   [38] L. Deweid, O. Avrutina, H. Kolmar, Microbial transglutaminase for
- biotechnological and biomedical engineering, Biol. Chem. 400 (3) (2019) 257–274.
- [39] M.K. McDermott, T. Chen, C.M. Williams, K.M. Markley, G.F. Payne, Mechanical properties of biomimetic tissue adhesive based on the microbial transglutaminasecatalyzed crosslinking of gelatin, Biomacromolecules 5 (4) (2004) 1270–1279.
- [40] C. Yung, et al., Transglutaminase crosslinked gelatin as a tissue engineering scaffold, J. Biomed. Mater. Res. A 83 (4) (2007) 1039–1046.
- [41] P.M. Crapo, T.W. Gilbert, S.F. Badylak, An overview of tissue and whole organ decellularization processes, Biomaterials 32 (12) (2011) 3233–3243.
- [42] R. Lennon, et al., Global analysis reveals the complexity of the human glomerular extracellular matrix, J. Am. Soc. Nephrol. JASN 25 (5) (2014) 939.
- [43] D. Wang, S. Sant, C. Lawless, N. Ferrell, A kidney proximal tubule model to evaluate effects of basement membrane stiffening on renal tubular epithelial cells, Integr. Biol. 14 (8–12) (2022) 171–183.
- [44] D. Venturoli, B. Rippe, Ficoll and dextran vs. globular proteins as probes for testing glomerular permselectivity: effects of molecular size, shape, charge, and deformability, Am. J. Physiol. Ren. Physiol. 288 (4) (2005) F605–F613.
- [45] C. Rippe, D. Asgeirsson, D. Venturoli, A. Rippe, B. Rippe, Effects of glomerular filtration rate on Ficoll sieving coefficients (θ) in rats, Kidney Int. 69 (8) (2006) 1326–1332.
- [46] J. Axelsson, K. Sverrisson, A. Rippe, W. Fissell, B. Rippe, Reduced diffusion of charge-modified, conformationally intact anionic Ficoll relative to neutral Ficoll across the rat glomerular filtration barrier in vivo, Am. J. Physiol. Ren. Physiol. 301 (4) (2011) F708–F712.
- [47] N. Ferrell, et al., Effects of pressure and electrical charge on macromolecular transport across bovine lens basement membrane, Biophys. J. 104 (7) (2013) 1476–1484.
- [48] W.H. Fissell, et al., Ficoll is not a rigid sphere, Am. J. Physiol. Ren. Physiol. 293 (4) (2007) F1209–F1213.
- [49] D. Wang, N. Ferrell, In vitro models to evaluate molecular permeability of the kidney filtration barrier. Kidney Research: Experimental Protocols, Springer, 2023, pp. 41–53.
- [50] J. Groszek, et al., Molecular conformation and filtration properties of anionic Ficoll, Am. J. Physiol. Ren. Physiol. 299 (4) (2010) F752–F757.
- [51] W.H. Fissell, C.L. Hofmann, R. Smith, M.H. Chen, Size and conformation of Ficoll as determined by size-exclusion chromatography followed by multiangle light scattering, Am. J. Physiol. Ren. Physiol. 298 (1) (2010) F205–F208.